

Antiulcer Agents. 5. Inhibition of Gastric H⁺/K⁺-ATPase by Substituted Imidazo[1,2-a]pyridines and Related Analogues and Its Implication in Modeling the High Affinity Potassium Ion Binding Site of the Gastric Proton Pump Enzyme

James J. Kaminski,*† Bjorn Wallmark,*‡ Carin Briving,† and Britt-Marie Andersson†

Department of Chemical Research, Schering-Plough Research, Schering-Plough Corporation, Bloomfield, New Jersey 07003, and Department of Biology, Hassle Gastrointestinal Research Laboratories, Molndal, Sweden. Received June 13, 1990

A number of substituted imidazo[1,2-a]pyridines and related analogues were selected for biochemical characterization in vitro against both the purified gastric proton pump enzyme, H⁺/K⁺-ATPase, and the intact gastric gland. The inhibitory activity in these two in vitro models was then examined for correlation with the gastric antisecretory potency determined for these compounds in vivo by using the histamine-stimulated Heidenhain pouch dog. Analysis of the biological data suggested that the inhibitory activity of the analogues determined in the two in vitro models is predictive of their in vivo gastric antisecretory activity following intravenous, but not oral, administration. Furthermore, the good correlation observed between the in vitro and in vivo models suggests that these compounds are gastric proton pump inhibitors in vivo. A molecular modeling study of these compounds using the *active analogue approach* has defined the molecular volume which is shared by the active analogues, as well as the molecular volume which is common to the inactive analogues. Graphical representation of the difference between these molecular volumes can be interpreted in terms of a hypothetical description of the pharmacophore by means of which 3-(cyanomethyl)-2-methyl-8-(phenylmethoxy)imidazo[1,2-a]pyridine, Sch 28080 (1) and its analogues interact with the gastric proton pump enzyme, H⁺/K⁺-ATPase.

The structure-activity relationship studies of a series of substituted imidazo[1,2-a]pyridines and related analogues which culminated with the identification and clinical advancement of 3-(cyanomethyl)-2-methyl-8-(phenylmethoxy)imidazo[1,2-a]pyridine, Sch 28080 (1) as an antiulcer agent exhibiting both gastric antisecretory and cytoprotective properties have been described.¹⁻³ In addition, definition of the interrelationship between the conformational characteristics of this series and their antiulcer activity, examined by using a variety of experimental and theoretical methods, led to the synthesis of *rigid* analogues which suggested a bioactive conformation for 1.⁴ Furthermore, it has recently been demonstrated that 1, the clinical prototype of this series, exerts its gastric antisecretory activity in its protonated form, by a kinetically competitive and reversible inhibition mechanism with respect to potassium ion in the extracellular domain of the gastric proton pump enzyme, H⁺/K⁺-ATPase.⁵

These observations prompted us to select a number of substituted imidazo[1,2-a]pyridines and related analogues for biochemical characterization, in vitro, in the purified gastric proton pump enzyme, H⁺/K⁺-ATPase, and the isolated intact gastric gland preparations. The inhibitory activity of these compounds determined in these two in vitro models could then be examined for correlation with their gastric antisecretory potency determined in vivo by using the histamine-stimulated Heidenhain pouch dog, following either intravenous or oral administration.

If an interrelationship exists between these in vitro and in vivo determined activities (vide infra), then a molecular modeling study of these selected compounds using the active analogue approach⁶⁻⁸ could define the pharmacophore and describe the active site of the enzyme where 1 and its analogues act.

The results of our biochemical and molecular modeling studies with these selected compounds constitute the subject matter of this report.

Chemistry

The syntheses of the compounds investigated in this report (Table I) have been described previously: 1 and 2, ref 1; 3 and 7-9, ref 2; and 4-6 and 10-12, ref 4.

Biological Test Methods. Gastric Antisecretory Activity. The compounds were evaluated for gastric antisecretory activity (Table I) by measuring their ability to inhibit histamine-stimulated gastric acid secretion in adult mongrel dogs with surgically prepared Heidenhain pouches as described previously.¹

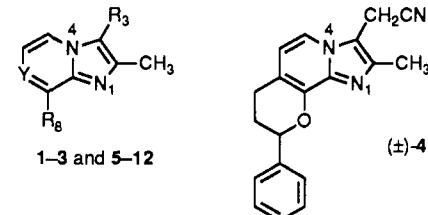
Compounds were administered intravenously (iv), 0.1-5 mg/kg, and orally (po), 2-8 mg/kg. The reduction in acid output relative to the non-drug-treated control value in the same animal was measured. The dose inhibiting histamine-stimulated gastric acid secretion by 50% (ED₅₀) was calculated by linear regression analysis. The range in parentheses indicates the confidence limits of the value determined at 95%.

Biochemical Activity. Inhibition of Purified H⁺/K⁺-ATPase. The compounds were evaluated for their ability to inhibit purified H⁺/K⁺-ATPase at pH 7.4 (Table I) by using gastric membrane vesicles prepared from hog stomach by differential and zonal density gradient centrifugation as previously reported.⁹ The ATPase activity

- (1) Kaminski, J. J.; Bristol, J. A.; Puchalski, C.; Lovey, R. G.; Elliott, A. J.; Guzik, H.; Solomon, D. M.; Conn, D. J.; Domalski, M. S.; Wong, S. C.; Gold, E. H.; Long, J. F.; Chiu, P. J. S.; Steinberg, M.; McPhail, A. T. *J. Med. Chem.* 1985, 28, 876.
- (2) Kaminski, J. J.; Hilbert, J. M.; Pramanik, B. N.; Solomon, D. M.; Conn, D. J.; Rizvi, R. K.; Elliott, A. J.; Guzik, H.; Lovey, R. G.; Domalski, M. S.; Wong, S. C.; Puchalski, C.; Gold, E. H.; Long, J. F.; Chiu, P. J. S.; McPhail, A. T. *J. Med. Chem.* 1987, 30, 2031.
- (3) Kaminski, J.; Perkins, D. G.; Frantz, J. D.; Solomon, D. M.; Elliott, A. J.; Chiu, P. J. S.; Long, J. F. *J. Med. Chem.* 1987, 30, 2047.
- (4) Kaminski, J. J.; Puchalski, C.; Solomon, D. M.; Rizvi, R. K.; Conn, D. J.; Elliott, A. J.; Lovey, R. G.; Guzik, H.; Chiu, P. J. S.; Long, J. F.; McPhail, A. T. *J. Med. Chem.* 1989, 32, 1686.
- (5) Briving, C.; Andersson, B.-M.; Nordberg, P.; Wallmark, B. *Biochim. Biophys. Acta* 1988, 946, 185, and references cited therein.
- (6) Humblet, C.; Marshall, G. R. *Annu. Rep. Med. Chem.* 1980, 15, 267.
- (7) Humblet, C.; Marshall, G. R. *Drug Dev. Res.* 1981, 1, 409.
- (8) Marshall, G. R. In *Macromolecular Structure and Specificity: Computer-assisted Modeling and Applications*, Venkataramhavan, B., Feldman, R., Ed., N. Y. Acad. Sci.: New York, 1985, p 162.
- (9) Saccomani, G.; Stewart, H. B.; Shaw, D.; Lewin, M.; Sachs, G. *Biochim. Biophys. Acta* 1977, 465, 311.

*Schering-Plough Research.

†Hassle Gastrointestinal Research Laboratories.

Table I. Gastric Antisecretory and Biochemical Activity of Substituted Imidazo[1,2-*a*]pyridines and Related Analogues


compd	Y	R ₃	R ₈	gastric antisecretory activity		biochemical activity				
				ED ₅₀ ^{iv} , mg/kg, ρ = 0.05	ED ₅₀ ^{po} , mg/kg, ρ = 0.05	gastric gland H ⁺ /K ⁺ -ATPase: IC ₅₀ , μmol/L	pK _a	purified H ⁺ /K ⁺ -ATPase		% protonated at pH 7.4
								IC ₅₀ , μmol/L	corrIC ₅₀ , μmol/L ^c	
1	HC	CH ₂ CN	PhCH ₂ O	0.09 (0.01-1.19) ^a	4.4 (2.1-14.0) ^a	0.065 ± 0.012	5.5 ^b	1.59 ± 0.4	0.0200	1.24
2	HC	CH ₂ CN	PhCH ₂ CH ₂	0.1 (approximate)	>4.4 (approximate)	0.13 ± 0.032	6.0 ^d	2.0 ± 0.7	0.0770	3.83
3	CH ₃ C	CH ₂ CN	PhCH ₂ O	0.53 (0.22-1.22) ^b	7.8 (3.2-38.3) ^b	0.40 ± 0.16	5.67	13.7 ± 0.73	0.2510	1.83
4	-	-	-	0.06 (0.02-0.14) ^c	3.7 (1.6-13.4) ^c	0.064 ± 0.002	6.0 ^d	0.092 ± 0.021	0.0035	3.83
5	HC	CH ₃	<i>E</i> -PhCH=CH	0.7 (0.06-2.6) ^e	4.8 (1.6-21.5) ^e	0.99 ± 0.457	7.2 ^d	1.68 ± 0.076	0.6500	38.70
6	HC	CH ₃	<i>E</i> -PhCH=CH	inactive ^e	inactive ^e	17.5 ± 5.3	7.2 ^d	28.4 ± 8.7	10.990	38.70
7	HC	NH ₂	PhCH ₂ O	0.1 (0.01-1.19) ^b	2.0 (approximate) ^b	0.31 ± 0.13	6.81 ^f	0.89 ± 0.066	0.1819	20.44
8	HC	NH ₂	PhCH ₂ CH ₂	1.0 (approximate)	6.7 (2.3-58.2)	1.46 ± 0.47	7.3 ^d	2.1 ± 0.07	0.9300	44.30
9	N	NH ₂	PhCH ₂ O	0.8 (0.2-6.0) ^b	1.4 (0.6-3.9) ^b	8.08	4.6 ^b	178	0.2800	0.158
10	HC	CH ₂ CN	<i>E</i> -PhCH=CHCH ₂	inactive ^e	inactive ^e	442 ± 23	6.0 ^d	206 ± 36	7.900	3.83
11	HC	CH ₂ CN	<i>E</i> -PhCH ₂ CH=CH	1.0 (approximate) ^e	4.0 (approximate) ^e	3.8 ± 1.2	5.70	14 ± 0.67	0.2700	1.96
12	HC	NH ₂	<i>E</i> -PhCH ₂ CH=CH	inactive ^e	inactive ^e	14.1 ± 5.4	6.75 ^d	8.6	1.5700	18.30

^aData obtained from ref 1. ^bData obtained from ref 2. ^cIC₅₀ values corrected for the percentage of test compound protonated at pH 7.4. ^dTheoretically calculated value, ref 17. ^eData obtained from ref 4, for analysis purposes an inactive compound is arbitrarily assigned an ED₅₀ value of 1000 μmol/kg. ^fpK_a value corrected from ref 2.

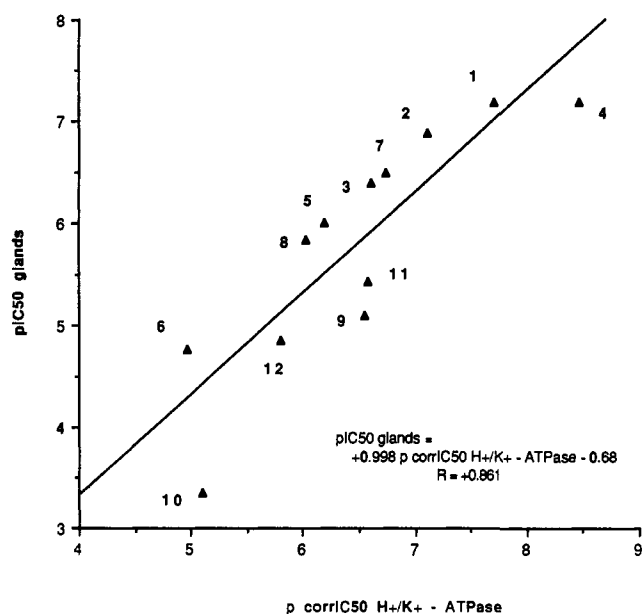
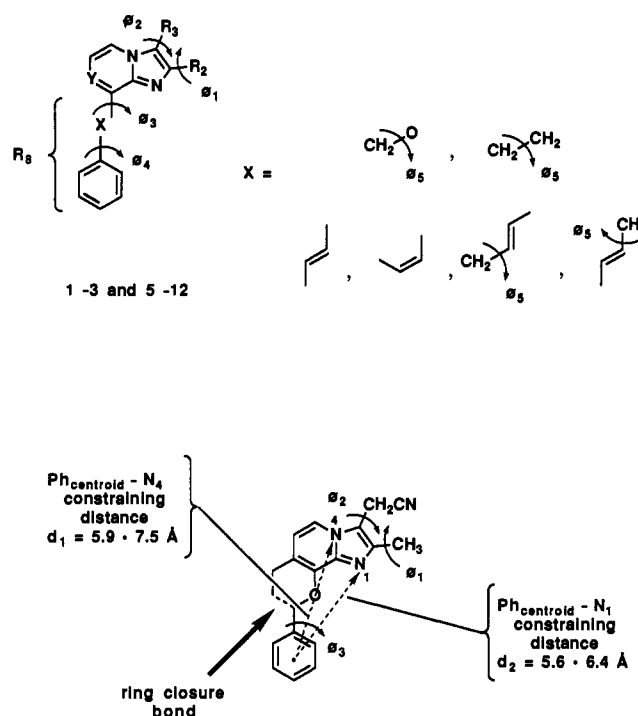


Figure 2. Correlation of the inhibitory potency of substituted imidazo[1,2-*a*]pyridines and related analogues corrected for the percent protonated at pH 7.4 in purified H⁺/K⁺-ATPase and isolated gastric glands.

was estimated as release of inorganic phosphate from ATP by using the method described by LeBel et al.¹⁰

Inhibition of H⁺/K⁺-ATPase in Gastric Glands. The compounds were evaluated for their ability to inhibit acid formation in rabbit gastric glands (Table I) as described previously.¹¹ Histamine-stimulated acid formation in the glands was monitored by uptake of the weak base aminopyrine.

The IC₅₀ values are defined as the drug concentration that gives 50% inhibition of K⁺-stimulated enzyme ac-



(±) 4 - R-isomer chosen for modeling

Figure 7. Conformational search variables for substituted imidazo[1,2-*a*]pyridines and related analogues. Rotatable bonds are designated as φ_n and ring-closure bond as (---).

tivity, or the drug concentration that gives 50% inhibition of the maximum stimulated aminopyrine accumulation. The IC₅₀ values were calculated by linear regression analysis and are expressed as IC₅₀ value ± standard error of the mean.

Protein was determined according to the method described by Bradford¹² with gammaglobulin as standard.

(10) LeBel, D.; Poirier, G. G.; Beaudouin, A. R. *Anal. Biochem.* 1978, 85, 86.

(11) Berglinth, T.; Obrink, K. J. *Acta Physiol. Scand.* 1976, 96, 150.

(12) Bradford, M. M. *Anal. Biochem.* 1976, 72, 428.

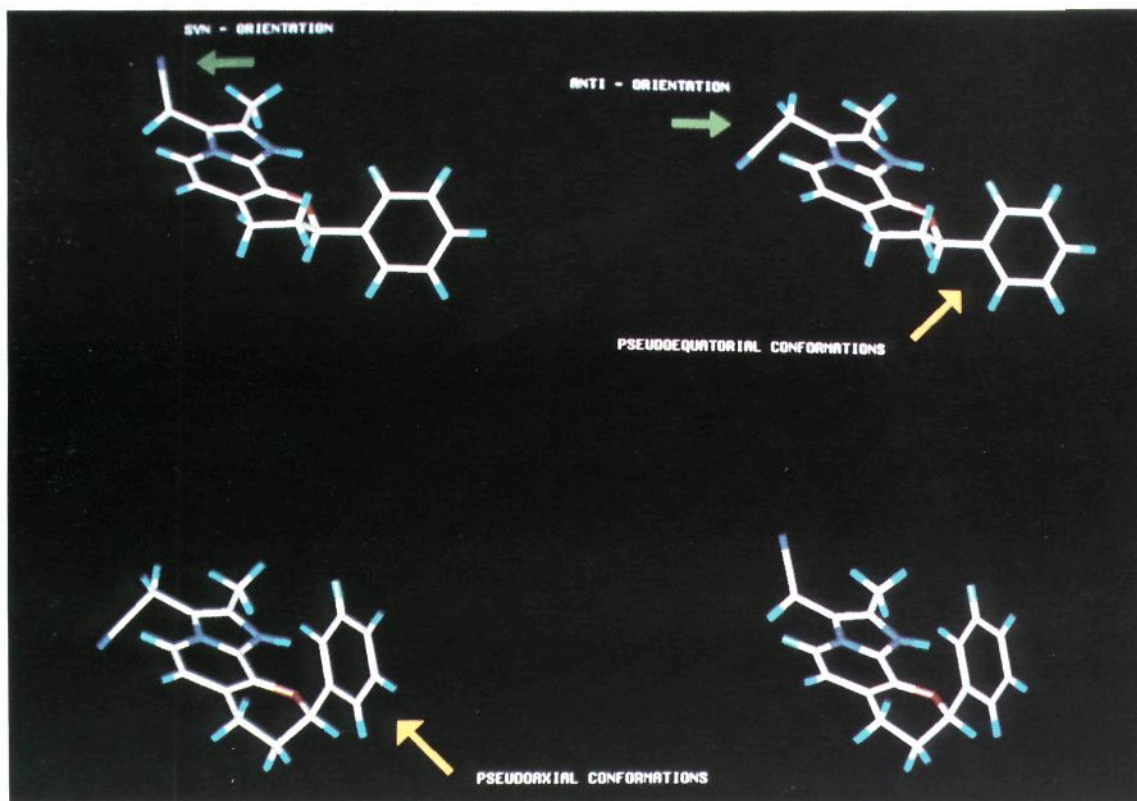


Figure 8. Valid conformations of 4 within +3.68 kJ/mol (~ 1 kcal/mol) of the global minimum energy conformation, conformation 1, $E = +97.92$ kJ/mol, of 4 (starting in the upper (right-hand corner and moving counter-clockwise); conformation 2, $E = +97.93$ kJ/mol; conformation 3, $E = +101.59$ kJ/mol; and conformation 4, $E = +101.60$ kJ/mol.

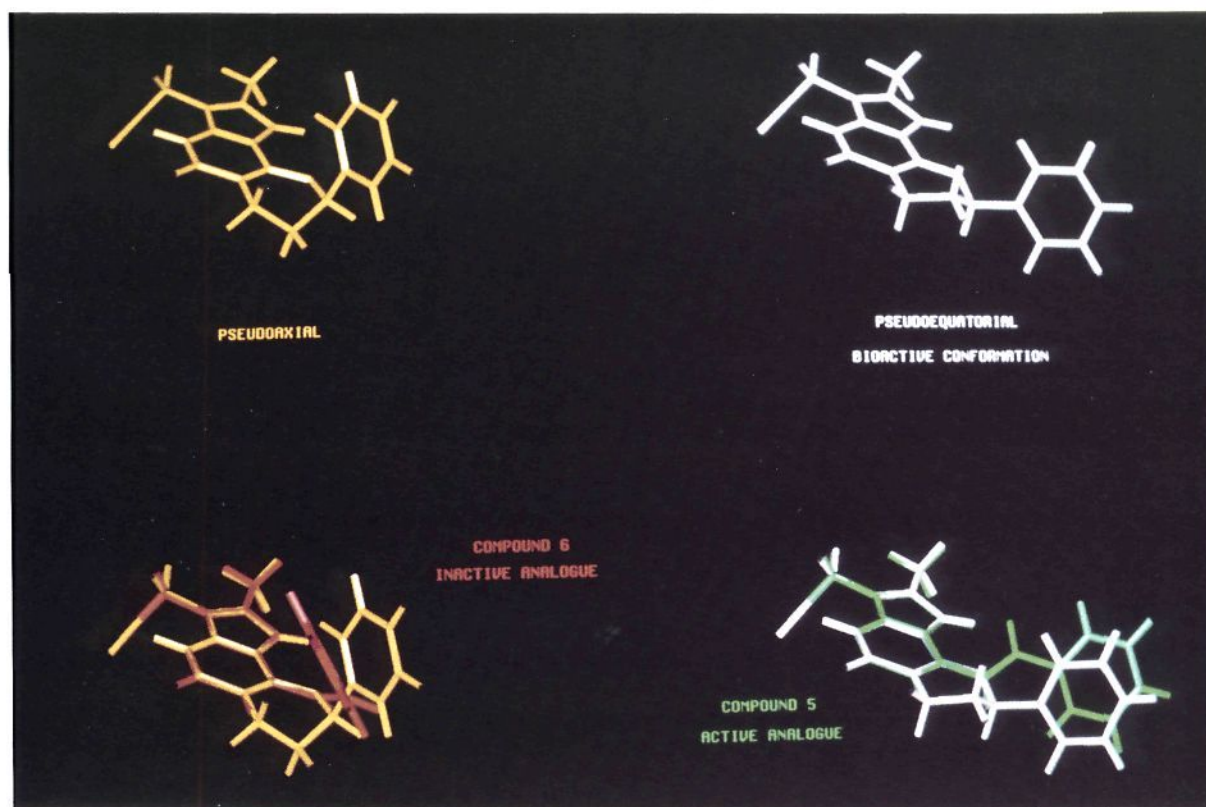


Figure 9. Comparison of the global minimum energy conformations of active analogue 5 and inactive analogue 6 with the pseudoequatorial and pseudoaxial conformations of 4. The global minimum energy conformation of 4, containing the pseudoequatorial phenyl group, best mimics the bioactive conformation for this series of substituted imidazo[1,2-a]pyridines and related analogues.

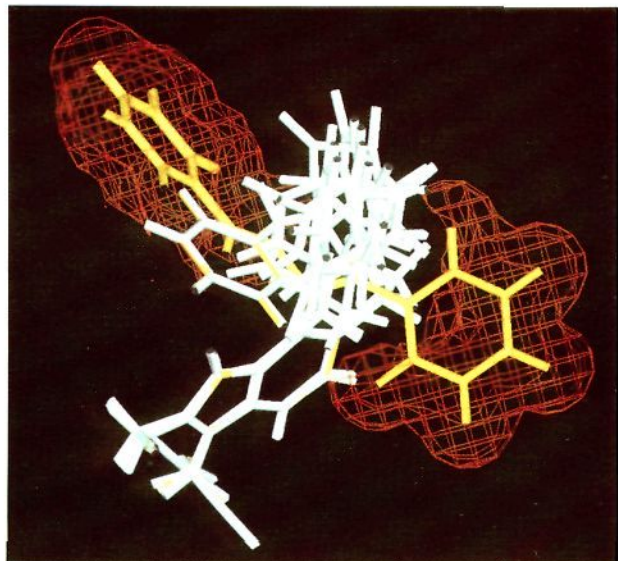


Figure 10. Conformations of the active analogues, 1–3, 7–9, and 11 (white), and the inactive analogues, 6, 10, and 12 (yellow) fit the minimum energy conformations of 4. The volume common to the inactive analogues, the excluded volume, is depicted in red. The molecules are compared by fitting the atoms of the imidazo[1,2-*a*]pyridine ring system by using the FIT command with SYBYL.

Molecular Modeling. Modeling studies of the compounds described in Table I were carried out with use of SYBYL Version 3.4¹³ and MacroModel V1.5.¹⁴

Results and Discussion. Biological Characterization of Substituted Imidazo[1,2-*a*]pyridines and Related Analogues. The *in vivo* gastric antisecretory and *in vitro* biochemical activity of the substituted imidazo[1,2-*a*]pyridines and related analogues are described in Table I. Graphical analyses of these biological data expressed as pX , where $pX = -\log [X]$, $X =$ biological data, suggest several interesting observations.

1. A good correlation exists between the inhibitory potency of the compounds in the *in vitro* isolated gastric gland and the purified enzyme model determined at pH 7.4. A plot of $pIC_{50}(\text{glands})$ versus $pIC_{50}(\text{H}^+/\text{K}^+\text{-ATPase})$ is linear with a slope approaching unity, $pIC_{50}(\text{glands}) = +0.98pIC_{50}(\text{H}^+/\text{K}^+\text{-ATPase}) + 0.65$, $r = +0.826$, Figure 1 (Supplementary Material).

Moreover, since it has been demonstrated that the prototype of this series, 1, exerts its inhibitory effect *in vitro* in its protonated form,⁵ a better correlation is obtained between the inhibitory potency of these compounds in the isolated gastric gland and purified enzyme model when correction is made for the percentage of compound existing in its protonated form at pH 7.4. The fraction of compound protonated at the solution pH of the purified enzyme assay can be determined from the relationship, $[\text{ImPH}^+]/[\text{ImP}] = 10^{-(\text{pH}-\text{p}K_a)} = 10^{-(7.4-\text{p}K_a)}$, where $[\text{ImPH}^+]$ refers to the concentration of the protonated form of the substituted imidazo[1,2-*a*]pyridine or related analogue, and $[\text{ImP}]$ refers to its concentration in the unprotonated form.

A plot of $pIC_{50}(\text{glands})$ versus $p^{\text{corr}}IC_{50}(\text{H}^+/\text{K}^+\text{-ATPase})$ is also linear with a slope approaching unity, and exhibiting

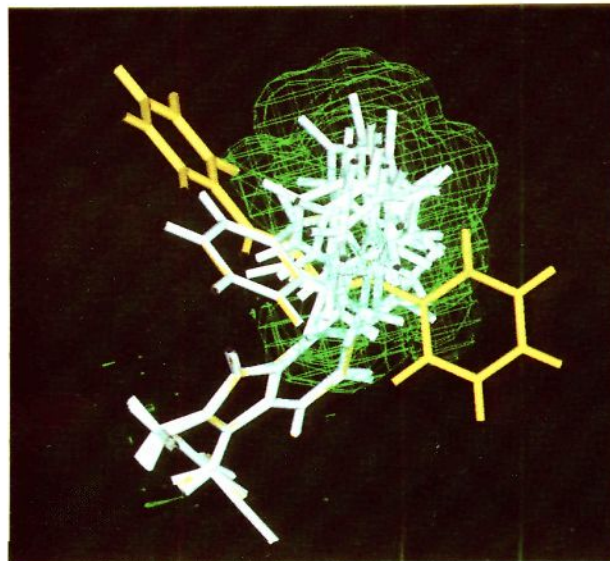


Figure 11. Conformations of the active analogues, 1–3, 7–9, and 11 (white), and the inactive analogues, 6, 10, and 12 (yellow) fit the minimum energy conformations of 4. The volume common to the active analogues, the included volume, is depicted in green. The molecules are compared by fitting the atoms of the imidazo[1,2-*a*]pyridine ring system by using the FIT command within SYBYL.

a marginally better correlation coefficient: $pIC_{50}(\text{glands}) = +0.998p^{\text{corr}}IC_{50}(\text{H}^+/\text{K}^+\text{-ATPase}) - 0.68$, $r = +0.861$, Figure 2.

2. The potency of the substituted imidazo[1,2-*a*]pyridines and related analogues as inhibitors of gastric acid secretion following intravenous administration correlates with the *in vitro* data determined in the isolated gastric gland, as well as with the *in vitro* data determined in the purified enzyme model, e.g. plots of pED_{50}^{iv} versus $pIC_{50}(\text{glands})$, and pED_{50}^{iv} versus $p^{\text{corr}}IC_{50}(\text{H}^+/\text{K}^+\text{-ATPase})$ are both linear, $pED_{50}^{\text{iv}} = +1.09pIC_{50}(\text{glands}) - 1.11$, $r = +0.889$, and $pED_{50}^{\text{iv}} = +1.24p^{\text{corr}}IC_{50}(\text{H}^+/\text{K}^+\text{-ATPase}) - 2.79$, $r = +0.868$, Figures 3 and 4, respectively (Supplementary Material). Thus, the correlations are linear with slopes close to unity.

3. Correlation of the oral potency of substituted imidazo[1,2-*a*]pyridines and related analogues to inhibit gastric acid secretion using data determined from either the isolated gastric gland, or the purified enzyme model is poor, e.g. plots of pED_{50}^{po} versus $pIC_{50}(\text{glands})$, and pED_{50}^{po} versus $p^{\text{corr}}(\text{H}^+/\text{K}^+\text{-ATPase})$ are linear and exhibit poorer correlation coefficients relative to the data determined following intravenous administration, $pED_{50}^{\text{po}} = +0.56pIC_{50}(\text{glands}) + 1.16$, $r = +0.738$ and $pED_{50}^{\text{po}} = +0.66p^{\text{corr}}IC_{50}(\text{H}^+/\text{K}^+\text{-ATPase}) + 0.16$, $r = +0.743$, Figures 5 and 6, respectively (Supplementary Material).

The poorer correlations observed following oral administration may be indicative of the different absorption, distribution, metabolism, and/or excretion profiles for each of the substituted imidazo[1,2-*a*]pyridines and related analogues investigated.

In summary, the observations described above suggest that the inhibitory activity of the substituted imidazo[1,2-*a*]pyridines and related analogues determined in the *two in vitro* models is predictive of their *in vivo* gastric antisecretory activity, following intravenous administration, in the histamine-stimulated Heidenhain pouch dog. Furthermore, the good correlation observed between the inhibitory activity determined in the *in vitro* and *in vivo*

(13) Tripos Associates, 1699 South Hanley Road, Suite 303, St. Louis, MO 63144.

(14) Still, W. C.; Mohamadi, F.; Richards, N. G. J.; Guida, W. C.; Lipton, M.; Liskamp, R.; Chang, G.; Hendrickson, T.; DeGunst, F.; Hasel, W. *MacroModel V1.5*, Department of Chemistry, Columbia University: New York, NY 10027.

models suggests that these compounds are gastric proton pump inhibitors in vivo.

Encouraged by these results, a molecular modeling study of the substituted imidazo[1,2-*a*]pyridines and related analogues using the active analog approach was initiated.

Molecular Modeling Studies of Substituted Imidazo[1,2-*a*]pyridines and Related Analogues. Selection of the substituted imidazo[1,2-*a*]pyridines and related analogues (1–12) for the molecular modeling study was based on an extensive investigation initiated to define the interrelationship between structure, antiulcer activity,^{1,2,4} and toxicology data³ derived from a series of compounds chosen from our structure–activity studies to identify a successor to 1.

Since all of the 2- and 3-substituents in 1–12 are fairly short and inflexible, and since the 2- and 3-positions are on the opposite side of the heterocyclic ring system from the 7- and 8-positions, the two groups of substituents for all practical purposes could be considered conformationally decoupled. On this basis, conformational analysis of 1–4, 10, and 11 could be simplified by replacing $R_3 = \text{CH}_2\text{CN}$ with CH_3 . However, it became apparent after introduction of a considerable number of 3-substituents with widely varying physical and chemical properties that the cyanomethyl group was almost uniquely effective in imparting the desired levels of oral antisecretory activity combined with cytoprotective action. In view of the *unconventional* nature of the cyanomethyl function, and its effect on pharmacologic activity, in concert with structural modifications at the 2-, 7-, and 8-positions, conformational analysis of 1–4, 10, and 11 with $R_3 = \text{CH}_2\text{CN}$ was conducted.

The results of modeling the substituted imidazo[1,2-*a*]pyridines and related analogues, 1–12, using SYBYL Version 3.4 and MacroModel V1.5 are summarized in Table II.

The molecular modeling study involved *three* distinct phases: (a) definition of the criteria and boundary conditions for the conformational searches of each of the substituted imidazo[1,2-*a*]pyridines and related analogues investigated, (b) reduction and analysis of the data derived from each of the conformational searches, and (c) hypothetical definition of the pharmacophore by means of which the substituted imidazo[1,2-*a*]pyridines and related analogues interact with the gastric proton pump enzyme, $\text{H}^+/\text{K}^+\text{-ATPase}$.

A synopsis of our results in each phase of the study is described below.

The substituted imidazo[1,2-*a*]pyridines and related analogues, 1–12, investigated in this study were created in MacroModel V1.5 by using the sketch facility or in SYBYL 3.4 by using molecular fragments obtained from the crystallographic fragment library available within SYBYL. Furthermore, since it has been established that it is the protonated form of these compounds that inhibits the enzyme, it was this form, protonation at N_1 , that was modeled rather than the free base. In any case, the molecular geometry of the initial conformation was minimized in MacroModel by using the MM2 force field and applying the block diagonal Newton–Raphson algorithm.¹⁵ The

energy is expressed in kJ/mol and the gradient first derivative root mean square (RMS) convergence criterion for the total energy of each initial conformation was ≤ 0.05 kJ/mol per Å (0.01 kcal/mol per Å), Table II.

Using the conformational search routine within SYBYL, a search of the gas-phase conformational hyperspace of 1–12 starting from, and including, each initial conformation and defined about the rotatable and ring-closure bonds¹⁶ described in Figure 7, was conducted. In each case, the incremental angle of rotation about the rotatable bonds was 30° , and the associated ranges of rotation were $0^\circ\text{--}119^\circ$ for attached methyl groups, $0^\circ\text{--}179^\circ$ for attached amino and phenyl groups, and $0^\circ\text{--}359^\circ$ for cyanomethyl groups and all other rotatable bonds in R_8 . The permitted variation in the distance between the ring closure atoms was modified to 0.25 Å, while the permitted variation in the valence angles about the ring-closure atoms were relaxed to 15° , Figure 7. All other ring-closure criteria used were the default values within SYBYL.

A. Definition of the Criteria and Boundary Conditions for the Conformational Searches. Initially, the conformational search of each substituted imidazo[1,2-*a*]pyridine and related analogue, 1–12, was examined invoking no energy calculations, charges or constraining distances. In addition, the default search criteria within SYBYL for van der Waals scaling factors were used, i.e. general VDW interaction/1.4 - interaction/hydrogen-bonding interaction = 0.95:0.87:0.65, respectively. Conformations that resulted from each search were examined for van der Waals contacts, and conformations that allowed two atoms to be closer to one another than the sum of their van der Waals radii were discarded. The total number of valid conformations (Σ_1) obtained for each molecule examined is described in Table II.

Using these search criteria, only 4, 5, and 6, from each search, gave a total number of valid conformations considered amenable to analysis, e.g. ≤ 1000 structures. The total number of valid conformations obtained were 880, 480, and 156, respectively. In all other cases examined, the total number of valid conformations obtained from each search significantly exceeded 1000 possibilities, approaching a maximum number of 12 230 valid conformations for 12. Since the central processing unit (CPU) time required to analyze such large datasets is clearly impractical, an alternative strategy was sought to reduce the number of conformations accessible to the remaining substituted imidazo[1,2-*a*]pyridines and related analogues.

Since 12 gave the greatest number of valid conformations possible when the initial search criteria was used, it was decided to use 12 to derive a set of boundary conditions which would maximize the number of valid conformations obtained from a conformational search of 12, and yet restrict the number of possibilities to ≤ 1000 structures. Once determined, these boundary conditions could be generally applied to the conformational searches of the remaining substituted imidazo[1,2-*a*]pyridines and related analogues. In order to retain the initial conformation, and reduce the total number of valid conformations obtained from the conformational search of 12 to ≤ 1000 structures, the search criteria determined were that the scaling factor for the 1,4 van der Waals interaction was optimum at a value of 1.00, the hydrogen-bonding interaction was kept

(15) Interaction between SYBYL and MacroModel was accomplished via the INTERFACE program. The INTERFACE program, [written by Dr. John W. Clader of the Schering-Plough Corporation] is a series of FORTRAN routines that effectively interchanges the formats and symbols used in SYBYL (mol and mol2) and MacroModel coordinate files. This program is available from Dr. John W. Clader, Schering - Plough Corporation, 60 Orange Stree, Bloomfield, New Jersey 07003.

(16) A *ring-closure bond* is a bond that is effectively removed or broken during a conformational search allowing torsion angles in the ring to freely rotate.

(17) Perrin, D. D.; Dempsey, B.; Serjeant, E. J. *pK_a Prediction for Organic Acids and Bases*; Chapman and Hall: London, England, 1981.

Table II. Molecular Modeling Study of Substituted Imidazo[1,2-*a*]pyridines and Related Analogues

cmpd	initial conformation ^a <i>E</i> (RMS)	Σ_1^b	VDW scaling factor ^c	Σ_2^d	MM2 SYBYL conf. _{min} ^e <i>E</i> (RMS)	BatchMin Σ_n^f				BatchMin constrained ^h		
						<i>n</i>	<i>E</i> _{min}	<i>E</i> _{max}	total	Σ_3^g	conf	<i>E</i> (RMS)
1	+98.99 (0.016)	3366	0.94	128	+95.81 (0.008)	2	+95.67	+95.82	4	128	1	+95.67 (0.028)
											2	+95.79 (0.028)
2	+85.29 (0.008)	2596	0.98	72	+78.71 (0.006)	2	+78.71	+85.19	12	24	1	+81.16 (0.027)
											2	+81.21 (0.032)
3	+107.91 (0.006)	10738	0.994	63	+87.98 (0.006)	2	+87.87	+87.99	4	7	1	+87.87 (0.032)
											2	+87.99 (0.027)
4	+97.92 (0.008)	880	-	-	-	-	-	-	-	-	1	+97.92 (0.031)
											2	+97.93 (0.031)
											3	+101.59 (0.033)
											4	+101.60 (0.033)
5	+99.23 (0.010)	480	-	-	-	1	+92.80	+99.12	7	276	1	+92.80 (0.031)
											2	+95.30 (0.031)
											3	+96.70 (0.026)
6	+108.96 (0.014)	156	-	-	-	1	+99.11	+108.96	4	12	1	+106.06 (0.035)
											2	+55.21 (0.029)
7	+58.51 (0.013)	7248	0.94	192	+55.26 (0.009)	2	+55.21	+55.27	2	192	1	+55.21 (0.029)
											2	+40.71 (0.029)
8	+44.83 (0.009)	5616	0.98	144	+38.85 (0.006)	2	+38.82	+44.67	8	48	1	+40.71 (0.029)
											2	+122.95 (0.039)
9	+122.92 (0.007)	8736	0.89	144	+122.96 (0.012)	2	+122.95	+122.95	2	144	1	+122.95 (0.039)
											2	+122.95 (0.033)
10	+89.20 (0.007)	5940	0.994	168	+89.05 (0.007)	2	+85.08	+89.57	16	48	1	+85.24 (0.043)
											2	+85.25 (0.042)
											3	+85.62 (0.034)
											4	+85.62 (0.034)
											5	+89.09 (0.038)
											6	+89.10 (0.038)
											7	+89.53 (0.034)
											8	+89.53 (0.030)
11	+90.68 (0.009)	4590	0.994	432	+86.95 (0.008)	2	+86.97	+93.46	26	64	1	+86.94 (0.031)
											2	+87.12 (0.034)
											3	+90.57 (0.028)
											4	+90.58 (0.038)
											5	+90.58 (0.038)
12	+50.24 (0.007)	12230	0.994	954	+46.40 (0.007)	2	+46.59	+53.00	11	106	1	+46.59 (0.038)
											2	+50.12 (0.042)

^a Molecule is minimized in MacroModel V1.5 by using the MM2 force field and applying the block diagonal Newton-Raphson algorithm. The energy is expressed in kJ/mol and the gradient first derivative root mean square (RMS) convergence criterion for the total energy of the initial conformation was ≤ 0.05 kJ/mol per Å (0.01 kcal/mol per Å). ^b Σ_1 represents the total number of valid conformations for a given molecule derived from the SYBYL 3.4 conformational search using the default search criteria within SYBYL, i.e. general VDW scaling factor/1,4-interaction/H-bonding interaction = 0.95:0.87:0.65, respectively. No energy calculations, distance constraints, or charges were invoked in the conformational search. ^c Variable value of the van der Waals scaling factor chosen such that the initial conformation is included in the conformational search. The 1,4- and hydrogen-bonding interactions were optimized, 1.00 and 0.65, respectively. In order to reduce the total number of valid conformations generated in the search to ≤ 1000 , it was necessary to invoke energy calculations, accepting all conformations 25 kcal/mol above the minimum energy conformation. No distance constraints were imposed in the conformational search, and charges associated with each molecule were calculated by using the Gasteiger-Marsili method. ^d Σ_2 represents the total number of valid conformations for a given molecule derived from the SYBYL 3.4 conformational search using the VDW scaling factor indicated and values for the remaining search criteria as described in footnote c above. ^e The energy of the minimum energy conformation identified from the SYBYL 3.4 conformational search minimized in MacroModel V1.5 by using the MM2 force field and applying the block diagonal Newton-Raphson algorithm. ^f BatchMin Σ_n represents the minimization of each of the valid conformations derived from each conformational search (Σ_n) in MacroModel V1.5 by using the MM2 force field and applying the block diagonal Newton-Raphson algorithm. The energy is expressed in kJ/mol and the gradient first derivative root mean square (RMS) convergence criterion for the total energy of each molecule was ≤ 0.05 kJ/mol per Å (0.01 kcal/mol per Å). The minimum energy conformation and those conformations 20 kJ/mol (~ 5 kcal/mol) above the minimum were stored. The energy of conformations E_{\min} and E_{\max} are reported as well as the total number of conformations retained after applying BatchMin. ^g Σ_3 represents the total number of valid conformations for a given molecule derived from repeating each Σ_2 SYBYL 3.4 conformational search, with the exception that distance constraints for the phenyl group, derived from the conformational search of 4, are imposed in the conformational searches of the other analogues, 1-3 and 5-12, $d_1 = 5.9-7.5$ Å and $d_2 = 5.6-6.4$ Å. ^h BatchMin constrained represents the minimization of each of the valid conformations derived from each constrained conformational search in MacroModel V1.5 by using the MM2 force field and applying the block diagonal Newton-Raphson algorithm. The energy is expressed in kJ/mol and the gradient first derivative root mean square (RMS) convergence criterion for the total energy of each molecule was ≤ 0.05 kJ/mol per Å (0.01 kcal/mol per Å). The minimum energy conformation and those conformations 20 kJ/mol (~ 5 kcal/mol) above the minimum were recorded.

at the 0.65 value, and the general VDW interaction was optimum at a value equal to 0.994. However, it was also necessary to invoke energy calculations, accepting all conformations within 25 kcal/mol above the minimum energy conformation. No distance constraints were invoked in the search, and charges associated with each molecule were calculated using the Gasteiger-Marsili method. By using these boundary conditions, the total number of valid conformations (Σ_2) obtained from the conformational search of 12 was 954.

For the remaining substituted imidazo[1,2-*a*]pyridines and related analogues, 1-3 and 7-11, conformational

searches were conducted with use of the boundary conditions described above for 12, with the exception that for each molecule examined, the general VDW interaction was allowed to vary and its value was optimized to produce the maximum number of valid conformations from each search, with an upper limit set at ≤ 1000 structures. The total number of valid conformations (Σ_2) obtained for each molecule examined is listed in Table II.

In all cases, the total number of valid conformations is significantly less than 1000. In addition, the conformational searches conducted with use of these boundary conditions and criteria identify and suggest a structure for

the minimum energy conformation determined by SYBYL.

B. Reduction and Analysis of the Data Derived from Each of the Conformational Searches. 1. Conformational Searches with and without Distance Constraints. SYBYL conformational searches utilizing energy rely on single-point energy estimates to retain or eliminate conformations from a search. Retention or dismissal of a conformation, in turn, depends upon the size of the energy window defined. Under these circumstances, it is possible that a conformation discarded on the basis of its high single-point determined energy may, in fact, minimize to a lower acceptable energy and conformation when completely relaxed. Therefore, it was decided that determination of the structure of the global minimum energy conformation from each conformational search described above might more accurately be reflected by minimization of each of the valid conformations derived from each conformational search. This task was easily accomplished by using the MacroModel batch minimizer (BatchMin) to analyze each of the SYBYL conformational searches.

Each of the valid conformations derived from each SYBYL conformational search (\sum_n , $n = 1$ or 2) was individually minimized by using the MM2 force field and applying the block diagonal Newton-Raphson algorithm. The energy is expressed in kJ/mol and the gradient first derivative root mean square (RMS) convergence criterion for the total energy of each molecule was ≤ 0.05 kJ/mol per Å (0.01 kcal/mol per Å). The minimum energy conformation and those conformations within 20 kJ/mol (~ 5 kcal/mol) of the minimum energy conformation were stored. The energy conformations E_{\min} and E_{\max} , as well as the total number of conformations retained after applying BatchMin, are reported in Table II.

In all cases, the total number of valid conformations retained is reduced, and the global minimum energy conformation determined after BatchMin processing of the data set is equal to, or lower, in energy than the starting conformation which was included in the conformational search. More importantly, minimization of the SYBYL-determined minimum energy conformation, using the MM2 force field and applying the block diagonal Newton-Raphson algorithm, results in a structure whose geometry and energy are *identical* with the BatchMin-determined global minimum energy conformation in all cases, excluding 10.

Constrained conformational searches for each of the substituted imidazo[1,2-*a*]pyridines and related analogues, 1-3 and 5-12, were also conducted by using the *unconstrained* conformational search criteria and boundary conditions defined above. The distance constraints invoked in each of the constrained searches relate to restriction of the conformational space made available to the phenyl group in each of the molecules investigated. The distance constraints applied (d_1 and d_2) were determined by the position of the phenyl group in the most potent (in vitro and in vivo) and conformationally constrained member of the series, 4, which has been suggested to define the bioactive conformation for this series, Figure 7.⁴ The total number of valid conformations (\sum_3) obtained for each molecule examined is listed in Table II.

In all cases, the total number of valid conformations obtained from each constrained conformational search is less than the total number of valid conformations obtained from its corresponding unconstrained search, as expected. Determination of the structure of the global minimum energy conformation using these search criteria and boundary conditions was also accomplished by using the

Table III. Conformations Allowed ($E_{\min} + 20$ kJ/mol) from the Constrained Conformational Searches of Each Substituted Imidazo[1,2-*a*]pyridine and Related Analogue FIT to the Minimum Energy Conformations of 4

compd	conformation	RMS, ^a Å	ΔE , ^b kJ/mol
1	1	0.0322	0
	2	0.0264	+0.12
2	1	0.0133	+2.45
	2	0.0068	+2.50
3	1	0.0312	0
	2	0.0253	+0.12
4	1	-	-
	2	0.0079	+0.01
5	1	0.0283	0
6	1	0.0077	+6.95
7	1	0.0307	0
8	1	0.0115	+1.89
9	1	0.0476	0
	2	0.0475	0
10	1	0.0050	+0.16
	2	0.0087	+0.17
11	1	0.0367	0
	2	0.0301	+0.15
12	1	0.0349	0

^aRoot mean square deviation (RMS) of fit, in Angstroms (Å), between each conformation and the minimum energy conformations of 4. The molecules are compared by fitting the atoms of the imidazo[1,2-*a*]pyridine (pyrazine) nuclei by using the FIT option within SYBYL 5.3. ^bThe energetic cost associated with the phenyl group in each substituted imidazo[1,2-*a*]pyridine or related analogue, adopting the orientation as in the minimum energy conformations of 4 from their respective minima, i.e. $\Delta E =$ constrained E_{\min} - unconstrained E_{\min} (kJ/mol).

MacroModel batch minimizer (BatchMin) to analyze each of the SYBYL conformational searches.

Each of the valid conformations derived from each constrained SYBYL conformational search (\sum_3) was individually minimized by using the MM2 force field and applying the block diagonal Newton-Raphson algorithm. The energy is expressed in kJ/mol and the gradient first derivative root mean square (RMS) convergence criterion for the total energy of each molecule was ≤ 0.05 kJ/mol per Å (0.01 kcal/mol per Å). The minimum energy conformation and those conformations within 20 kJ/mol (~ 5 kcal/mol) of the minimum energy conformation were recorded (Table II).

Identical conformational searches conducted with and without distance constraints defining a proposed bioactive conformation allow assessment of the energetic cost that inactive compounds would have to incur in order to adopt the proposed bioactive conformation, i.e. $\Delta E =$ constrained E_{\min} - unconstrained E_{\min} (kJ/mol).

For active compounds, 1-3, 5, 7-9, and 11, it was found that there was no significant energetic cost associated with the phenyl groups' adopting the conformation of the phenyl group of 4 (0-2.45 kJ/mol, 0-0.6 kcal/mol), while for inactive compound 6, the energetic cost was 6.95 kJ/mol, 1.7 kcal/mol (Table III). Although an energetic cost of 1.7 kcal/mol appears to be modest, entropic penalties not considered in the computation of ΔE can also contribute substantially to the overall energy required for the phenyl group of 6 to adopt the bioactive conformation and can therefore affect its activity.

For example, analogues 10, 11, and 12 exhibit no significant energetic cost for their phenyl groups to adopt the conformation of an active compound ($\Delta E = \sim 0$ kJ/mol, 0 kcal/mol). However, 10, 11, and 12 also contain an additional atom in the R_3 substituent separating the phenyl group from the imidazo[1,2-*a*]pyridine nucleus. The presence of this additional atom introduces an additional degree of freedom (ϕ_6) for the phenyl group in 10,

11, or 12, which is not available to the phenyl group in 6. Consequently, the energetic and entropic effects influencing activity may be greater in 6 than in 10, 11, or 12, yet analogue 11 is active, while analogues 10 and 12 are not.

The apparent inconsistencies observed between the activity of these analogues and the energetic requirements to adopt the bioactive conformation can be resolved by considering their respective intrinsic activity as measured by the rank ordering of their potency against the purified H⁺/K⁺-ATPase enzyme corrected for the percent protonated at pH 7.4. The ^{corr}IC₅₀ (μmol/L) for 6, 10, 11, and 12 is 10.99, 7.90, 0.27, and 1.57, respectively. This observation suggests that relative to the most potent and conformationally constrained member of this series, analogues 6, 10, 11, and 12 are approximately 3000×, 2000×, 75×, and 500× intrinsically less potent than 4, respectively. Therefore, while attainment of the bioactive conformation may be necessary, it is clearly not a sufficient criterion alone to determine the activity of these analogues, especially for those analogues containing a 3-atom fragment between the imidazo[1,2-*a*]pyridine ring and the phenyl group.

The pK_a of the analogue, and its effect in determining the concentration of the protonated species, which is the active form at the site of action in the parietal cell, can clearly dominate any predicted activity based on conformational considerations alone.

Encouraged by our ability to rationalize these results on the basis of all available experimental and theoretical data, the active analogue approach was applied to these compounds to define the pharmacophore where the substituted imidazo[1,2-*a*]pyridines and related analogues act.

C. Hypothetical Definition of the Pharmacophore by Means of Which Substituted Imidazo[1,2-*a*]pyridines and Related Analogues Interact with the Gastric Pump Enzyme, H⁺/K⁺-ATPase. An unconstrained search of the conformational hyperspace of 4 about the rotatable and ring-closure bonds defined in Figure 7 resulted in a total number of 880 valid conformations Σ₁, (Table II). When each of these valid conformations was individually minimized by using the MM2 force field and applying the block diagonal Newton-Raphson algorithm, there were identified four conformations of 4 within 3.68 kJ/mol (~1 kcal/mol) of the global minimum (Table III). These four conformations of 4 consist of two sets that differ from each other only by the ring conformation that the phenyl-substituted dihydropyrano ring adopts that is fused to the imidazo[1,2-*a*]pyridine ring system (yellow arrows, Figure 8).

Furthermore, within each set, the two conformations are within 0.01 kJ/mol (0.002 kcal/mol) of each other, and differ only by the orientation of their 3-cyanomethyl group with respect to the phenyl substituent, being directed either above (syn), or below (anti), the plane of the imidazo[1,2-*a*]pyridine ring (green arrows, Figure 8).

Since 4 has been proposed to mimic the bioactive conformation for this series⁴ (Figure 9) the minimum energy conformations allowed from the constrained conformational searches of each substituted imidazo[1,2-*a*]pyridine and related analogue were compared to the minimum energy conformations of 4 (Table III). The various conformations were compared by fitting the atoms of the imidazo[1,2-*a*]pyridine nuclei by using the FIT command within SYBYL. In all cases, the root mean square (RMS) deviation of fit, in Angstroms (Å), between each conformation and the minimum energy conformations of 4 was <0.05 Å.

By using the compared structures described above, the total molecular volume of the active analogues, 1-5, 7-9, and 11, and the total molecular volume of the inactive analogs, 6, 10, and 12, were generated by using the MVO-LUME command within SYBYL (vide infra). The total molecular volumes are based on the minimum energy conformations obtained from each constrained search for each substituted imidazo[1,2-*a*]pyridine and related analogue (Table III).

By difference, the molecular volume shared by the inactive analogues, as well as the molecular volume common to the active analogues was visualized, Figures 10 and 11, respectively. Graphical representation of the excluded and included molecular volume maps can be interpreted as a hypothetical description of the pharmacophore whereby 1 and its analogues interact with the gastric proton pump enzyme, H⁺/K⁺-ATPase. This model may be useful for the prospective design and qualitative evaluation of structurally related and/or novel gastric proton pump, H⁺/K⁺-ATPase, inhibitors which share the same mechanism of action.

In conclusion, it has been demonstrated that the inhibitory activity of the substituted imidazo[1,2-*a*]pyridines and related analogues determined in vitro against the purified gastric proton pump enzyme, H⁺/K⁺-ATPase, and the intact gastric gland is predictive of their in vivo gastric antisecretory activity, following intravenous administration, in the histamine-stimulated Heidenhain pouch dog. In addition, the good correlation between the inhibitory activity determined in the in vitro and in vivo models suggests that these compounds are gastric proton pump inhibitors in vivo.

Furthermore, a molecular modeling study of these selected compounds using the active analogue approach has generated an hypothetical, graphical representation of the pharmacophore by means of which 1 and its analogues interact with the gastric proton pump enzyme, H⁺/K⁺-ATPase.¹⁸

Experimental Section

Biology. Purified H⁺/K⁺-ATPase. Gastric membrane vesicles containing H⁺/K⁺-ATPase were prepared from hog stomach by differential and zonal gradient centrifugation according to previously published methods⁹ with the following modifications. The density gradient was prepared accordingly: 100 mL of 8.5% sucrose, 200 mL of 7.5% Ficoll in 8.5% sucrose, and 300 mL of 30% sucrose, all three solutions in 2 mM Pipes adjusted to pH 7.4 with Trizma base. The membrane fraction was fractionated above the Ficoll interface was designated the GI fraction and was employed in these studies.

The GI fraction was diluted with 2 mM Pipes-Tris (pH 7.4) to obtain a 1% sucrose concentration and recentrifuged at 100000g. The resulting pellets were suspended in 2 mM Pipes-Tris (pH 7.4) and subsequently lyophilized and stored at -20 °C until use. The final lyophilization step rendered these vesicles permeable to K⁺ such that the stimulation of ATPase activity by K⁺ at the luminal (intravesicular) site did not require a K⁺-transporting ionophore.

Gastric Glands. Isolated gastric glands were prepared from rabbits as previously described.¹¹ The minced gastric corpus mucosa from one rabbit was digested with collagenase at 37 °C for about 1 h. After digestion, the glands were rinsed three times and resuspended in respiratory medium (RM) to a concentration of 80 mg wet weight/mL. Collagenase medium (CM) pH 7.4 12 250 units of collagenase (type IA, Sigma) was dissolved in 50 mL of a medium, pH 7.4 containing (mM): NaCl 130, NaHCO₃ 12.0, NaH₂PO₄ 3.0, Na₂HPO₄ 3.0, K₂HPO₄ 3.0, MgSO₄ 2.0, CaCl₂ 1.0,

(18) A forthcoming paper will discuss the comparative molecular field analysis (CoMFA) for these substituted imidazo[1,2-*a*]pyridines and related analogues with respect to their in vitro inhibition of the gastric proton pump enzyme, H⁺/K⁺-ATPase, and their in vivo gastric antisecretory activity.

indomethacin 0.01, *N*- α -tosyl-L-lysine chloromethyl ketone 0.1, glucose 2 mg/mL, and albumin 2 mg/mL. Respiratory medium (RM) pH 7.4 contained (in mM NaCl 132.5, KCl 5.4, MgCl₂ 1.2, CaCl₂ 1.0, NaH₂PO₄ 1.0, Na₂HPO₄ 5.0, indomethacin 0.01, glucose 2 mg/mL, and albumin 2 mg/mL.

Inhibitors. For the *in vitro* experiments the inhibitor, substituted imidazo[1,2-*a*]pyridines, and related analogues, 1-12, were dissolved and diluted in methanol. Aliquots were pipetted into the incubation media. The final methanol concentration was 1%, which had no effect on the enzyme or the gland preparations.

Methods. Determination of the H⁺/K⁺-ATPase Activity. Membrane vesicles (10 μ g) and inhibitor were preincubated for 30 min in 2 mM Pipes-Tris (pH 7.4) and 10 mM KCl at 37 °C. An ATP solution was added to give a final concentration of 2 mM ATP and 2 mM MgCl₂. The ATPase activity was estimated as release of inorganic phosphate from ATP.¹⁰ K⁺-stimulated activity was obtained by subtracting the basal Mg²⁺ activity from the enzyme reaction in the presence of K⁺ and Mg²⁺. The effect of the highest concentration of each inhibitory compound on the recovery of a standard amount of inorganic phosphate was also determined.

Determination of Acid Formation in Gastric Glands. Acid formation was monitored by uptake of the weak base aminopyrine.¹¹ In a final volume of 2500 μ L, 10 mg (wet weight) of glands were incubated in polypropylene vials. The incubation medium was RM containing 0.05 μ Ci [¹⁴C]aminopyrine. Incubations were carried out at 37 °C in a shaker bath for 1 h and secretagogue activation by the addition of 10⁻⁴ M histamine.

Protein Determination. Protein was determined according to the method described by Bradford,¹² with use of the Bio-Rad Protein Assay kit. Bovine gammaglobulin was used as a standard.

Molecular Modeling. Computational Procedures. All molecular modeling was performed with use of an Evans and Sutherland PS350 tethered to a μ VAXII serving as a host machine. Conformational analyses were conducted by using the SEARCH subroutine within SYBYL 3.4 using the search criteria and boundary conditions described in Table II.

Energy minimizations were conducted in MacroModel V1.5 by using the MM2 force field and applying the block diagonal Newton-Raphson algorithm. The energy is expressed in kJ/mol and the gradient first derivative root mean square (RMS) convergence criterion of the total energy of the molecule was ≤ 0.05 kJ/mol per Å (0.01 kcal/mol per Å). The minimum energy conformation and those conformations within 20 kJ/mol (~ 5 kcal/mol) of the minimum were recorded.

Interaction between SYBYL 3.4 and MacroModel V1.5 was accomplished via the INTERFACE program.¹⁵

Molecules were compared by using the FIT command within SYBYL as described.

Finally, the molecular database containing the compared molecules was ported to a Silicon Graphics 4D/240 acting as a server. Molecular volumes were generated from the logical combination of molecules by using the MVOLUME command within SYBYL 5.3. The total molecular volume of the active analogues, 1-5, 7-9, and 11, was obtained from the arithmetic sum of the molecular volume of each conformation for each active analogue described in Table III. Likewise, the total molecular volume of the inactive analogues, 6, 10, and 12, was obtained from the arithmetic sum of the molecular volume of each conformation for each inactive analogue described in Table III. The excluded and included molecular volumes were obtained by applying the difference operator to the arithmetic sums of the active and inactive molecular volumes described above, i.e. excluded volume = (inactive - active) volumes and included volume = (active - inactive) volumes.

Graphical representation of the molecular volumes was visualized and recorded by using SYBYL 5.3 on a Silicon Graphics 4D/120 workstation.

Acknowledgment. We thank Dr. John W. Clader of the Schering-Plough Corporation for developing and making available to us the INTERFACE program, and Dr. Arne Brandstrom of AB Hassle for providing the theoretical pK_a values for various substituted imidazo[1,2-*a*]pyridines and related analogues. We also thank Dr. Robert E. Carter of AB Hassle for his comments in reviewing the manuscript. We are especially grateful to Dr. Daniel M. Solomon for many valuable discussions throughout the course of this work, and for providing his expertise in photography.

Registry No. 1, 76081-98-6; 2, 91848-84-9; 3, 91848-94-1; 4, 130883-17-9; 5, 85542-20-7; 6, 85345-71-7; 7, 85333-23-9; 8, 85333-50-2; 9, 85333-46-6; 10, 121394-23-8; 11, 85332-63-4; 12, 121394-24-9; ATPase, 9000-83-3.

Supplementary Material Available: The data and Figures 1 and 3-6, describing the correlations between the *in vitro* biochemical activity and the *in vivo* gastric antisecretory activity of substituted imidazo[1,2-*a*]pyridines and related analogues, and SYBYL 5.3 MOL files for the conformations described in Table III (83 pages). Ordering information is given on any current masthead page.

Synthesis, Peroxidating Ability, and Antineoplastic Evaluation of 1-[(Aminoalkyl)amino]-4-hydroxy-10-imino-9-anthracenones

Maria Dzieduszycka,[†] Sante Martelli,[‡] Jolanta Tarasiuk,[†] Jolanta Paradziej-Łukowicz,[†] and Edward Borowski^{*†}

Department of Pharmaceutical Technology and Biochemistry, Technical University of Gdańsk, 80-952 Gdańsk, Poland, and Department of Chemical Sciences, University of Camerino, 62032 Camerino (MC), Italy. Received January 31, 1990

A novel group of cytotoxic anthraquinone derivatives, 1-[(aminoalkyl)amino]-4-hydroxy-10-imino-9-anthracenones, has been synthesized. It has been shown that imino analogues of the anthracenediones exhibit diminished ability to generate oxygen radicals. The cytotoxic activity of iminoanthracenones obtained was lower than that of the related quinone carbonyl analogues. One of the obtained imino compounds showed a moderate antileukemic activity *in vivo*.

Among the most clinically useful intercalating agents against human malignancy are the anthracycline antibiotics daunorubicin (DR) and adriamycin (ADR) (1a and 1b, Chart I). Their utilization is, however, limited by

undesired effects such as irreversible cardiotoxicity.¹ Several studies have suggested that anthracyclines cardiotoxicity may be associated with the mediation by anthraquinone drugs of the formation of reactive oxygen species and subsequent cellular lipid peroxidation.²

* To whom the correspondence should be addressed.

[†] Technical University of Gdańsk.

[‡] University of Camerino.

(1) (a) Banadonna, G.; Monfardini, S. *Lancet* 1969, 1, 837. (b) Lenaz, L.; Page, J. A. *Cancer Treat. Rev.* 1976, 3, 111.